Journal of Applied Pharmaceutical Research
Volume 14 Issue 3, Year of Publication 2026, Page 345 – 354
DOI: https://doi.org/10.69857/joapr.v14i3.1987

Check for updates

Research Article

JOURNAL OF APPLIED PHARMACEUTICAL RESEARCH | JOAPR
www.japtronline.com ***ISSN: 2348 – 0335***

FORMULATION AND COMPARATIVE EVALUATION OF ALLOPURINOL TRANSDERMAL PATCHES USING TWO DIFFERENT POLYMERIC COMBINATIONS

Adity Modak[1], Tiyash Roy[1,2], Abhishek Jana[1,3], Swarnim Gupta[1,3], Pintu Kumar De[1]*

Article Information
Received: 3rd February 2026
Revised: 19th March 2026
Accepted: 20th April 2026
Published: 15th May 2026

Keywords
Allopurinol, Transdermal, Gout, Drug delivery, hydrophilic polymer.

ABSTRACT

Background: The transdermal drug delivery system is a technique where drugs are absorbed via the skin at a predetermined and controlled rate. This system offers several benefits over conventional routes, such as intravenous or oral administration, for both systemic and local drug delivery, and it is simple to administer. This technique is also painless. The goal of the dosage model for transdermal medications is to simultaneously enhance drug efflux from the skin into the systemic circulation while minimizing drug metabolism and retention in the skin. The selected drug for the present formulation is Allopurinol, a xanthine oxidase inhibitor that lowers uric acid levels in the body. **Methodology:** The goal of this study is the development of a matrix-type transdermal system of allopurinol with two different hydrophilic polymers, polyethylene glycol-4000(PEG-4000) and hydroxyl propyl methyl cellulose (HPMC), along with a hydrophobic polymer, Ethyl cellulose (EC), in different ratios by using the solvent evaporation technique to create a suitable matrix-type patch. **Results and Discussion:** The physicochemical characterization of thickness, folding endurance, moisture content, and drug-polymer compatibility has been studied. The drug release studies from the formulation, P1F3, showed maximum release of allopurinol (59.43%) in 5 h, where EC: PEG-4000 was 2:1; whereas P2F3 showed maximum release of allopurinol (57.28%) in 5 hours, where EC: HPMC was 2:1. In both cases, the release rate is retarding by increasing the proportion of hydrophobic polymer EC. **Conclusion:** The physicochemical evaluation of the prepared transdermal patches revealed good physical stability, with controlled drug release achieved by varying the ratios of hydrophilic and hydrophobic polymers.

INTRODUCTION

In Western nations, the prevalence of gout is high (between 1% to 20%), making it the most common kind of inflammatory arthritis. Additionally, during the past 20 years, the prevalence of gout in the USA has about doubled, with people over 65 experiencing the highest increase. Monosodium urate crystals (MSU) deposit in tissues, causing the systemic illness known as gout [1]. For uric acid crystals to develop, serum uric acid (SUA)

[1]*Department of Pharmaceutical Technology JIS University, Kolkata, West Bengal- 700109, India.*
[2]*Dr. Sudhir Chandra Sur Institute of Pharmaceutical Science and Technology, Kolkata, West Bengal- 700074, India.*
[3]*JIS Institute of Pharmacy, Kalyani, Nadia, West Bengal- 741235, India*

For Correspondence: **pintu.de@jisuniversity.ac.in**

levels must rise over a particular threshold. An important requirement for the onset of gout is an increase in serum uric acid (SUA) levels, often known as hyperuricemia. Monosodium urate (MSU) crystals form and deposit in and around joints as SUA levels rise and the natural saturation threshold of uric acid in body fluids is exceeded [2].

Clinical signs of MSU crystal deposition include tophaceous deposits of MSU crystals in the joints and skin, chronic joint deterioration, and sudden bouts of excruciating pain and inflammation affecting peripheral joints, most frequently the first metatarsophalangeal (MTP) joint, persistent joint injury, tophaceous MSU crystal deposits in the joints and skin, and metatarsophalangeal (MTP) joint. There are two basic types of anti-gout drugs that can be used in different conditions. The first kind helps reduce pain and swelling caused by gout attacks [3]. The second type lowers blood uric acid levels to avoid gout complications. Gout is treated with medications that reduce the production of uric acid. The level of uric acid produced in the body can be reduced with medications such as febuxostat (Uloric) and allopurinol. Uric acid elimination can be enhanced with drugs like probenecid. Allopurinol (ALP) is a xanthine oxidase inhibitor and the first-line medication for treating hyperuricemia and gout.

It functions by inhibiting xanthine oxidase, the enzyme that produces uric acid. ALP has the drawback of being insoluble in both aqueous and acidic conditions, despite being the first-line treatment. Due to hepatic metabolism, ALP also has a reduced half-life of 1-2 hours. Both factors lower ALP's bioavailability, thereby reducing its treatment options. ALP also causes gastrointestinal side effects. Additionally, ALP is linked to neurological symptoms (pain, sleepiness), gastrointestinal side effects (diarrhea, vomiting), and hypersensitivity (fever, malaise, abnormalities in liver function, and kidney failure) [4]. The main focus of this study is to deliver ALP transdermally to overcome ALP-associated drawbacks and achieve localized delivery. In this study, a matrix-type transdermal therapeutic system for ALP is fabricated using a solvent-evaporation technique [5]. A variety of polymers with different ratios, solvents, and plasticizers are used. Infrared spectroscopy has been used to assess the physicochemical compatibility and interactions between the polymers and the drug. Several physical and chemical evaluation tests have been conducted. *In vitro drug-release and ex vivo skin-permeation studies were also conducted* [6]. This study will help identify the optimal polymer combination for formulating an ALP-loaded patch.

MATERIALS AND METHODS

Materials

Free samples of ALP were obtained from Lincoln Pharmaceuticals in Ahmedabad, India. Polyethylene glycol 4000 (PEG), hydroxyl propyl methyl cellulose (HPMC), ethyl cellulose (EC), polyvinyl alcohol, and dibutyl phthalate were supplied by local suppliers. The investigation also used acetone, chloroform, potassium dihydrogen phosphate, disodium hydrogen phosphate, and other analytical-grade substances. For every research technique, double-distilled water was utilized.

Formulation of Allopurinol Transdermal Patch

Using various ratios of hydrophobic and hydrophilic polymers, EC [7] with PEG4000 or HPMC [6], prepared by the solvent evaporation technique [8], matrix-type transdermal patches containing allopurinol have been developed. After that, the polymers from each combination were weighed in the appropriate ratio and dissolved in a solvent. The drug was then added to the homogenous dispersion by slowly stirring with a magnetic stirrer for 45 minutes after the plasticizer (30% of the total polymer weight) was added, as shown in Table 1 [9]. The PVA (4% w/v) backing membrane was coated with the homogeneous dispersion. A funnel was placed over the Petri dish to regulate the evaporation rate, and the solvent was left to evaporate for a full day at room temperature. They were stored in desiccators for additional research after drying [10], [11].

Table 1: Formulation table of different Allopurinol transdermal patches

F Code	API(mg)	EC (mg)	PEG4000 (mg)	HPMC(mg)	Acetone(ml)	Chloroform(ml)	Dibutyl Pthalate (%)
P1F1	50	375	375	-	-	10	30
P1F2	50	250	500	-	-	10	30
P1F3	50	500	250	-	-	10	30
P2F1	50	300	-	300	10	-	30
P2F2	50	200	-	400	10	-	30
P2F3	50	400	-	200	10	-	30

Fourier transform infrared (FT-IR) spectroscopy

Infrared spectroscopy of the pure drug sample and the drug-polymer physical admixture was performed to identify any incompatibility. The observed peaks corresponding to various functional groups were compared with those reported in [12] and [13].

Physical appearance

Every transdermal patch formulation was visually examined for color, clarity, air-bubble entrapment, flexibility & smoothness [14].

Thickness

A digital micrometer was used to assess the thickness of the transdermal patch [15].

Weight variation

10 randomly chosen transdermal patches were weighed individually, and the average weight was determined. Patches' individual weights should not vary considerably from the average weight [16].

Flatness

Five randomly chosen transdermal films of each formulation were divided into longitudinal strips. One from the patch's center and one from its opposite side. Each strip's length was measured. 100% flatness was defined as 0% constriction [17]. By measuring the strip's constriction using the provided formula, flatness was determined.

$$\% \, \boldsymbol{Constriction} = \left[\frac{\boldsymbol{L1 - L2}}{\boldsymbol{L1}}\right] \times \mathbf{100}$$

Where L_1= Initial length of each strip, L_2 = Cut film length.

Folding endurance

To measure the folding endurance of patches, a small patch strip (about 2 × 2 cm) was repeatedly folded at the same spot until it broke. The value of folding endurance was determined by counting how many times patches could be folded at the same spot without breaking [18].

Moisture content

Transdermal patches were weighed separately and stored in a desiccator filled with calcium chloride for 24 hours at room temperature to determine their moisture content. The transdermal patches were weighed several times until their weights stabilized. The formula below was used to determine the moisture content [19] [20].

$$\%\boldsymbol{MoistureContent} = \left[\frac{\boldsymbol{FinalWeight - InitialWeight}}{\boldsymbol{Initial}}\right] \times \mathbf{100}$$

Moisture uptake

Transdermal patches were weighed (Ws) after being kept in desiccators at room temperature for 24 hours with silica gel. They were then transferred to different desiccators to be exposed to 75% RH using a saturated sodium chloride solution at 25°C. The patches were then repeatedly weighed until a consistent weight (Wm) was achieved. Using the provided formula, the moisture uptake capacity was determined [21].

$$\%\boldsymbol{Moistureuptakecapacity} = [\frac{\boldsymbol{Wm - Ws}}{\boldsymbol{Ws}}] \times \mathbf{100}$$

Drug Content

One area (7,065 cm2) of transdermal membrane should be cut into small pieces, dissolved in 50ml of phosphate buffer (pH 6.8), and sonicated for 5 minutes. Whatman filter paper was used to filter the chemical sample, and a 100 ml volumetric flask was filled with the filtrate. After that, phosphate buffer at pH 6.8 was added to bring the volume to 100 ml. Take 1 ml of the solution above and dilute it with phosphate buffer (pH 6.8) to a final volume of 100 ml. Measurements of absorbance are made at 250nm [22].

***In-vitro* drug release studies**

The drug release from the transdermal patches is evaluated in this investigation using the USP apparatus II at 50 rpm. Here, pH 6.8 phosphate buffer is used. The volume of the media was 900 ml, and 5ml of the sample was withdrawn at different time intervals up to 5 hrs. The samples were filtered, and absorbance was measured using a spectrophotometer [23], [24].

Drug release kinetics

The release is calculated using kinetic models such as Higuchi's model (cumulative percentage of drug released vs. the square root of time), zero-order (cumulative amount of drug released vs. time), and first-order (log of the cumulative percentage of drug remaining vs. time)[25].

Scanning Electron Microscopic study

The surface morphology of the patch was studied before and after permeation studies using scanning electron microscopy [28].

***Ex vivo* skin permeation study**

P1F1 and P2F1 were selected as the optimized formulations based on the physicochemical characterization results,

particularly the drug-release profile. A skin permeation study was carried out using hairless pig ear skin. The patch was kept in contact with the stratum corneum of the skin mounted on the Franz diffusion cells [26], [27].

RESULT AND DISCUSSION

Fourier transform infrared spectroscopy(FT-IR)

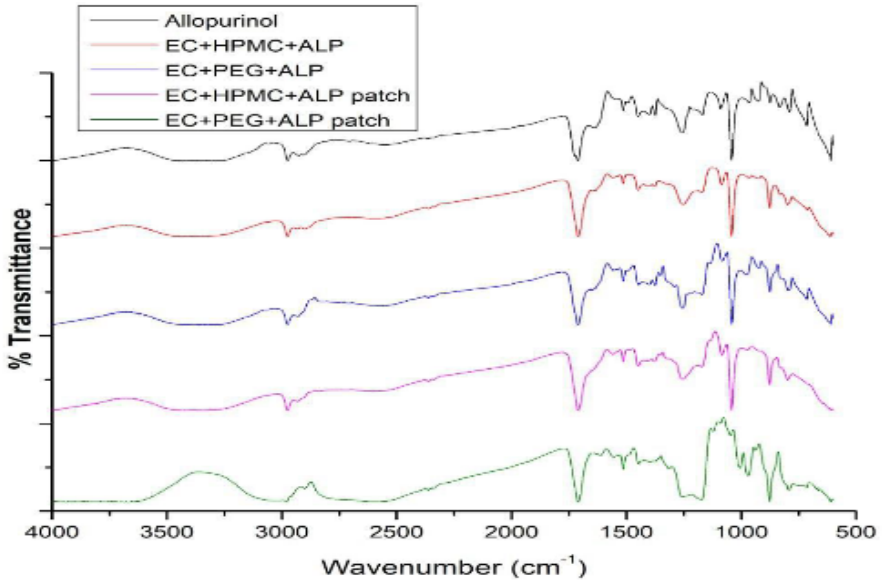

Figure 1: FTIR spectroscopy of allopurinol, HPMC, EC, and PEG-4000 physical admixtures and transdermal films.

Table 2: Different formulations' data table for folding endurance, drug content, weight variation, thickness, flatness, moisture content, and moisture uptake

F. Code	FE	DC (%)	WV (mg)	Thickness (mm)	Flatness (%)	MC	Moisture uptake
P1F1	207±0.63	92.8±0.58	465.93±1.4	0.148±0.002	100	6.43±0.67	6.94 ±0.7
P1F2	231±0.47	91.3 ±0.72	453.07±2.3	0.126±0.005	100	8.14±0.35	7.19 ± 0.5
P1F3	224±0.79	89.7±0.65	441.85±1.5	0.107±0.003	100	3.16±0.52	5.46 ± 0.4
P2F1	210±0.60	93.6±0.55	359.86±1.5	0.156±0.004	100	7.28±0.66	5.85 ±0.55
P2F2	241±0.52	90.8 ±0.69	354.05±2.1	0.133±0.003	100	9.20±0.41	8.16 ± 0.48
P2F3	235±0.84	88.7±0.63	345.90±1.2	0.115±0.002	100	5.10±0.50	4.89± 0.6

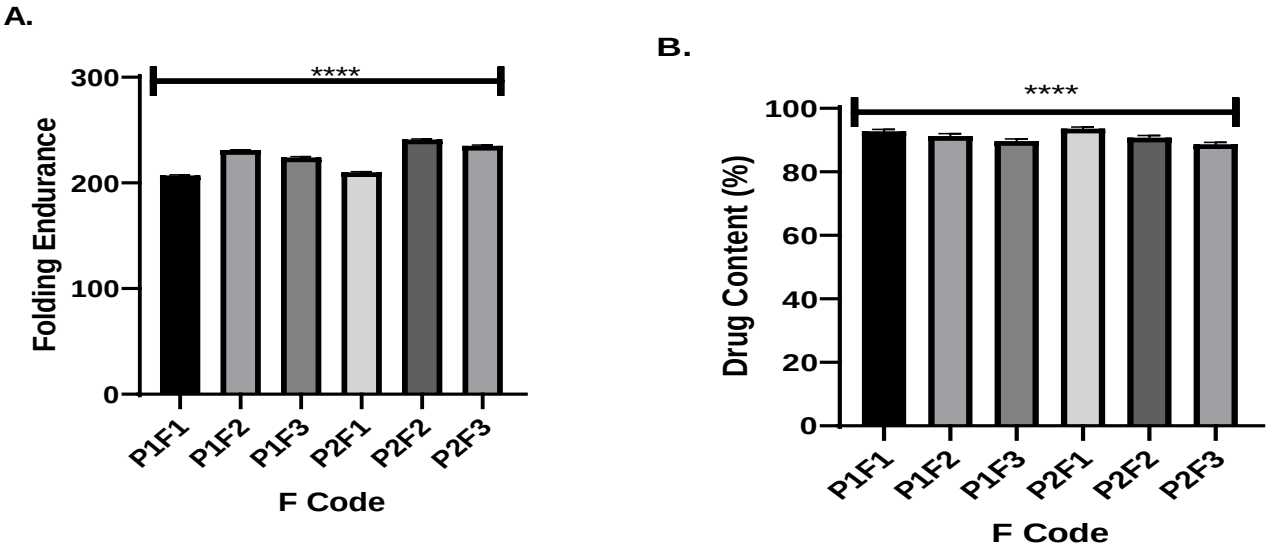

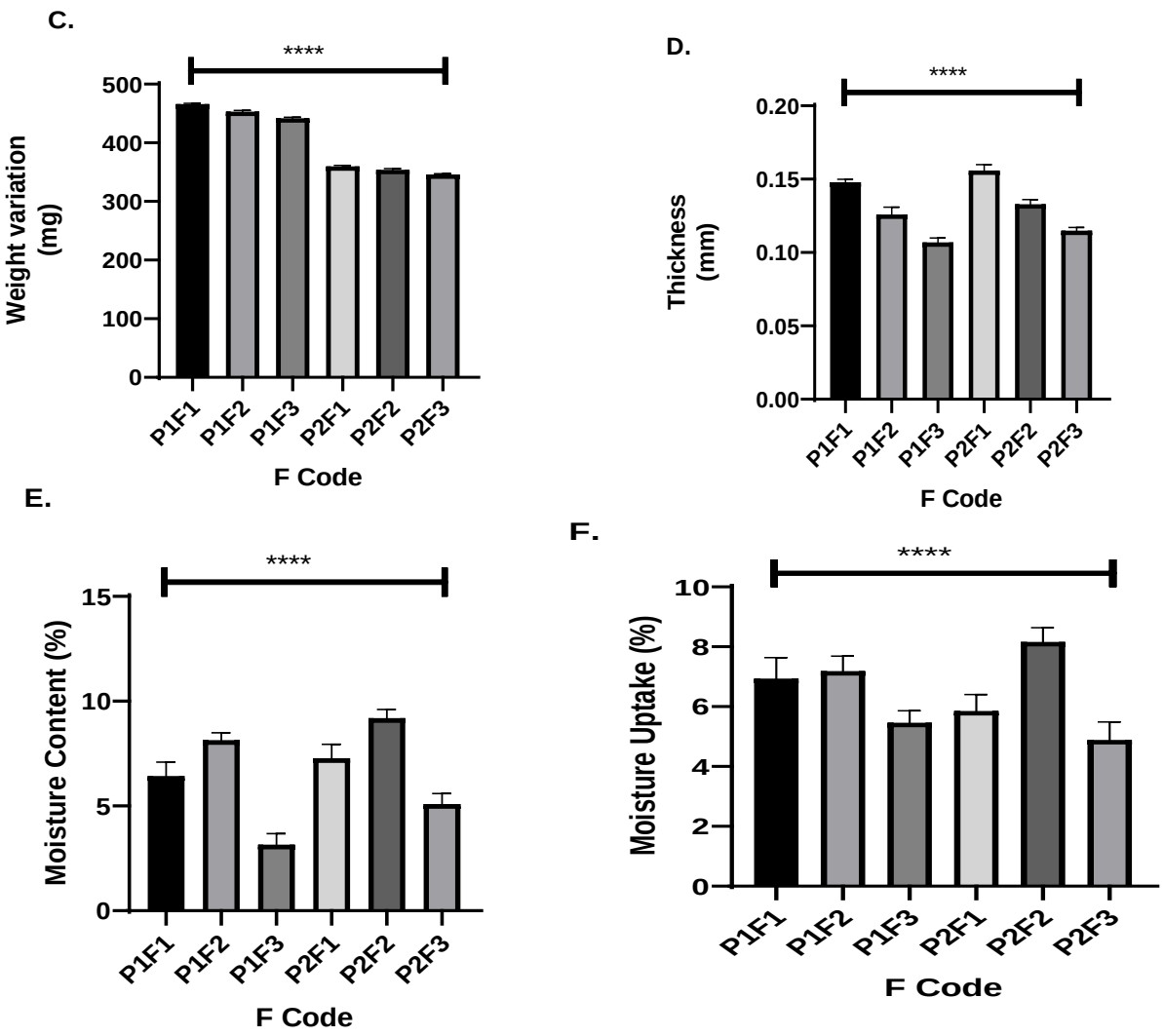

Figure 2: ANOVA Analysis of A. Folding Endurance B. Drug Content (%) C. Weight variation (mg) D. Thickness (mm) E. Moisture Content (%) F. Moisture uptake (%) with p values, "**" denotes P value <0.0001, which ensures Significance**

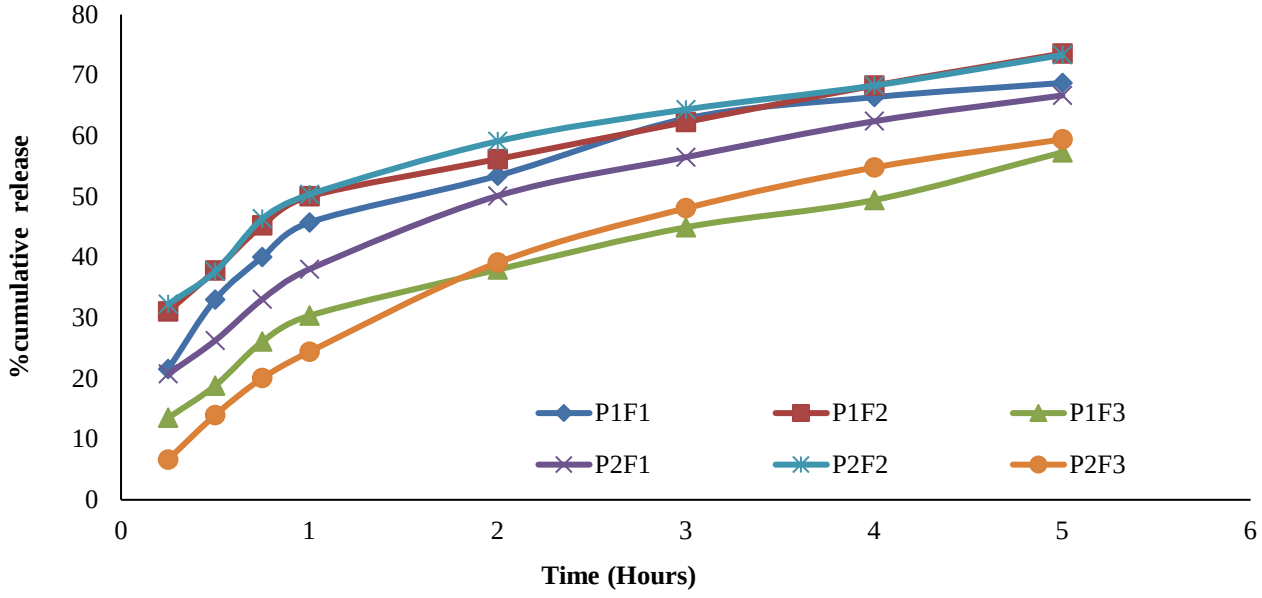

Figure 3: Release pattern of different transdermal formulations of allopurinol in pH 6.8

Drug release kinetics

Table 3: Release kinetics of transdermal patches of allopurinol

F Code	Zero order	1st Order	Higuchi	Korsmeyer–Peppas	
	R^2	R^2	R^2	R^2	n
P1F1	0.863	0.932	0.95	0.942	0.48
P1F2	0.943	0.975	0.987	0.975	0.55
P1F3	0.917	0.971	0.974	0.972	0.45
P2F1	0.93	0.974	0.987	0.979	0.58
P2F2	0.941	0.978	0.992	0.989	0.62
P2F3	0.89	0.949	0.967	0.952	0.59

***Ex vivo* permeation study of Allopurinol patch**

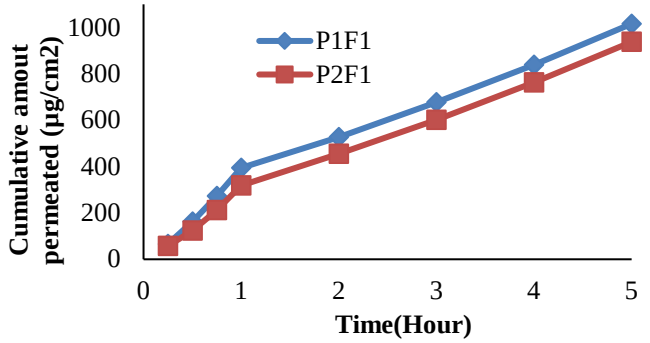

Figure 4: *Ex vivo* permeation comparison between P1F1 and P2F1 formulation

Scanning electron microscopic study

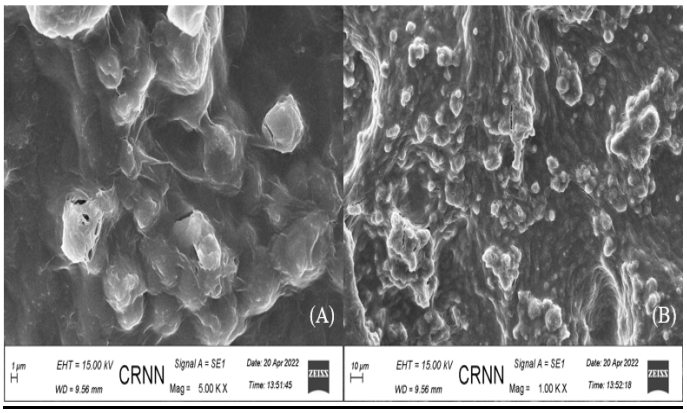

Figure 5: SEM picture of Allopurinol patch surface indicating presence of drug particles, (A) zoom in and (B) zoom out

DISCUSSION

Fourier transform infrared spectroscopy(FT-IR)

To confirm the physicochemical compatibility between the drug and the formulation excipients, infrared spectra of Allopurinol and its physical mixtures with EC, PEG4000, and HPMC were recorded. Allopurinol's infrared spectra revealed a distinctive peak at 3178,3178,3078 cm-1 (Aromatic CH stretching), 1700 cm-1 (C=O stretching), 1586 cm-1 (N-H stretching), 1482 cm-1 (C=N stretching), 1378 cm-1 (C=C stretching), and 1237 cm-1 (C-N stretching). Allopurinol's distinctive peaks were clearly visible in the infrared spectra of the physical mixture (allopurinol, EC, and PEG4000 or HPMC), and a slight shift in their positions suggested no drug-polymer interaction. However, due to the polymer, additional peaks were also observed in the physical mixture. Hence, the drug and polymers can be successfully incorporated in the formulation shown in Figure 1 [29], [30].

Folding Endurance

P1F1 has the lowest folding endurance (207±0.63), and P2F2 has the best folding endurance (241±0.52), according to a manual measurement. The findings in Table 2 showed that patches from all batches would not break and would remain intact when applied with typical skin folding [31].

Drug Content (%)

No significant difference in drug content was observed among all the formulated patches, which ranged from 88.7±0.63 (P2F3) to 93.6±0.55 (P2F1). The results in Table 2 indicate that the method used to prepare the patch achieved uniform drug content due to the homogeneous dispersion of the drug [32], [33].

Weight variation

The weight of the patches ranged from 345mg (P2F3) to 465mg (P1F1), indicating that the prepared patches exhibit minor weight variation. Here, P1F1 and P2F1 show more weight variation due to containing a high amount of PEG4000 and HPMC; similarly, P1F3 and P2F3 show less weight variation due to a low amount of PEG4000 and HPMC, as shown in Table 2 [34].

Thickness

The thicknesses of different batches ranged from 0.107±0.003 to 0.156±0.004. A low standard deviation in the film thickness measurements indicates the uniformity of the patches shown in Table 2 [35].

Flatness

To determine the formulation's construction, flatness investigations were conducted. All formulated patches were 100% flat, indicating no restriction, as shown in Table 2 [36].

Moisture Content

The moisture content ranges from 3.16±0.52 to 9.20±0.41. The results shown in Table 2 indicate that the hydrophilicity of the polymers is directly proportional to the % moisture contents [37]. The patches containing PEG4000 show a higher % moisture content than those containing HPMC.

Moisture uptake

The moisture content ranges from 4.89± 0.6 to 8.16 ± 0.48. The results shown in Table 2 indicate that the hydrophilicity of the polymers is directly proportional to the % moisture uptake. The patches containing PEG4000 show a higher % moisture content than those containing HPMC. Similar results have been reported by other researchers [38].

***In-vitro* drug release studies of Allopurinol patches**

Over 5 hours, the cumulative drug release from formulations P1F1, P1F2, and P1F3 was 68.73%, 73.58%, and 59.43%, respectively. Over 5 hours, the total drug release from formulations P2F1, P2F2, and P2F3 was 66.66%, 73.33%, and 57.28%, respectively. The highest % drug release (73.58%) was observed in formulation P1F2, which was significantly greater than the lowest value (57.28%) observed in formulation P2F3. From the in vitro drug release study, we found that as polymer hydrophilicity increases, the percentage of drug released also increases, as shown in Figure 3. Apart from that, the data trend also indicates that HPMC provides better drug retention capacity than PEG 4000 [39], [40].

Drug release kinetics

The Higuchi equation was the best kinetic model for this formulation, although the plots showed strong linearity, with the highest R2 values reported in Table 3, indicating diffusion. However, n values ranging between 0.45 and 0.62 indicate anomalous (non-Fickian) diffusion. The formulation's ability to provide matrix-type drug dispersion was therefore verified [41].

***Ex vivo* skin permeation study**

The ex vivo permeation study was conducted using full-thickness dorsal skin from a hairless pig ear (Skin thickness was approximately 0.8–1.0 mm; the stratum corneum side faced the donor compartment). The Allopurinol transdermal patch was kept adhered to the stratum corneum of the skin mounted on the Franz diffusion cells. For P1F118.45%, the drug was permeated after 15 min, and after 60 min, the permeation is about 34.89%, and at the end of 5 hours, ' time 64.19% of the total drug was permeated. Similarly, for P2F1, after 15 min, the drug permeated by 17.89%; after 60 min, it was about 34.98%; and after 5 hours, it was about 34.98%. At time 64.01%, 64.01% of the total drug has permeated. So, the data clearly indicate in Figure 4 that the formulations provide sustained drug release and a prolonged drug flux with proper permeation capacity [42], [43], [44].

The ex vivo permeation study demonstrated that approximately 64% of Allopurinol permeated through the skin within 5 hours, indicating sustained and efficient drug transport across the membrane. Allopurinol is commonly administered orally at doses of 100–300 mg/day to manage gout and maintain therapeutic plasma uric acid levels [45]. The permeation profile observed in the present study suggests that the developed transdermal patch can provide controlled, sustained drug delivery, which may help maintain plasma concentrations within the therapeutic range while potentially reducing gastrointestinal adverse effects associated with oral administration. Transdermal drug delivery systems are designed to enable continuous drug transport across the skin barrier, thereby maintaining relatively stable plasma drug levels and improving patient compliance compared to conventional dosage forms [46,47]. In matrix-type transdermal patches, drug release generally occurs via diffusion from the polymeric matrix, followed by permeation across the skin, thereby enabling prolonged drug release and controlled therapeutic delivery [48]. The permeation behavior observed in this study, therefore, indicates that the developed formulation has the potential to achieve therapeutically relevant drug delivery via the transdermal route. However, since the present work primarily focused on formulation development and in vitro/ex vivo evaluation, further pharmacokinetic and in vivo studies are required to determine the exact therapeutic flux and confirm clinical efficacy for gout management [49].

Scanning electron microscopic study of Allopurinol patch

Scanning electron microscopy (SEM) was employed to examine the surface morphology of the developed transdermal patches before and after the in-vitro permeation study using a Franz diffusion cell [50]. The SEM micrographs revealed a smooth, compact, and continuous polymeric surface, indicating successful film formation and proper integration of the polymers within the matrix. Such morphology is typical of well-formed polymeric transdermal systems designed for controlled drug delivery [51,52].

Closer observation of the micrographs revealed small particulate structures distributed throughout the matrix, which may represent drug crystals or drug-rich domains formed during solvent evaporation due to differences in drug–polymer solubility and drug migration toward the film surface [52]. Despite these minor surface features, the overall morphology indicates uniform dispersion of Allopurinol within the ethyl cellulose-based polymeric matrix, confirming successful drug incorporation.

The compact polymer network observed in the SEM images is characteristic of matrix-type transdermal systems, in which drug release occurs predominantly by diffusion from the polymeric matrix [53]. The presence of limited numbers of surface-localized drug particles may contribute to a slight initial burst release upon contact with the release medium, followed by sustained diffusion-controlled drug release from the polymer matrix, consistent with the reported release behavior of matrix-type transdermal patches [54].

CONCLUSION

Using various combinations of hydrophilic and hydrophobic polymers, matrix-type transdermal patches containing Allopurinol have been effectively developed. The FTIR study shows the absence of drug-excipient interaction, and physicochemical characterization confirms the patch's suitability for long-term use. The drug release profile and *ex vivo* skin permeation study showed differences in the drug release rate and the amount permeated per unit area of skin. Both polymer combinations are useful for controlled drug delivery and sustained action.

FINANCIAL ASSISTANCE

NIL

CONFLICT OF INTEREST

The authors declare no conflict of interest.

AUTHOR CONTRIBUTION

The contributions of the authors are as follows: Adity Modak was responsible for conceptualization, methodology, and writing. Tiyash Roy contributed to methodology, data analysis, writing, and editing. Abhishek Jana's contributions included data analysis, writing, and editing. Swarnim Gupta provided support in writing and editing. Pintu Kumar De was involved in conceptualization and supervision.

REFERENCES

[1] Ali Z, Din FU, Zahid F, Sohail S, Imran B, Khan S, Malik M, Zeb A, Khan GM. Transdermal delivery of allopurinol-loaded nanostructured lipid carrier in the treatment of gout. *BMC Pharmacol Toxicol*, **23(1)**, 86 (2022) https://doi.org/10.1186/s40360-022-00625-y

[2] Wang R, Wang H, Jiang G, Sun Y, Liu T, Nie L, Shavandi A, Yunusov KE, Aharodnikau UE, Solomevich SO. Transdermal delivery of allopurinol to acute hyperuricemic mice via polymer microneedles for regulation of serum uric acid levels. *Biomater Sci*, **11(5)**, 1704–1713 (2023) https://doi.org/10.1039/D2BM01836E

[3] Khan M, Kanwal M. Advances in transdermal delivery of zolmitriptan and frovatriptan: pharmacology, therapeutic challenges, and innovative strategies. *J Med Health Sci Rev*, **2(4)** (2025) https://doi.org/10.65035/3tk2k466

[4] Sikandar M, Shoaib MH, Yousuf RI, Ahmed FR, Siddiqui F, Saleem MT, Irshad A. Dissolving microneedle patches for transdermal delivery of paroxetine: in-vitro, ex-vivo studies and PBPK modeling. *Ther Deliv*, **16(9)**, 835–851 (2025) https://doi.org/10.1080/20415990.2025.2542721

[5] Shelke PV, Rachh PR, Mankar SD, Prasad LG. Optimization and evaluation of transdermal delivery system for nebivolol hydrochloride. *J Appl Pharm Res*, **12(3)**, 21–37 (2024) https://doi.org/10.69857/joapr.v12i3.580

[6] Shafique M, Ur Rehman M, Kamal Z, Alzhrani RM, Alshehri S, Alamri AH, Bakkari MA, Sabei FY, Safhi AY, Mohammed AM, Hamd MA. Formulation development of lipid polymer hybrid nanoparticles of doxorubicin and its in-vitro, in-vivo and computational evaluation. *Front Pharmacol*, **14**, 1025013 (2023) https://doi.org/10.3389/fphar.2023.1025013

[7] Sabbagh F, Kim BS. Recent advances in polymeric transdermal drug delivery systems. *J Control Release*, **341**, 132–146 (2022) https://doi.org/10.1016/j.jconrel.2021.11.025

[8] Jamaludin WB, Muthia R, Kartini K, Setiawan F, Juhrah S, Yulida N. Formulation and evaluation of transdermal patches from *Eleutherine bulbosa* bulb extract with plasticizer variations. *Int J Appl Pharm*, **16(1)**, 94–97 (2024)

[9] Halder S, Chakraborty P, Pradhan D, Bagchi A. Recent advancement in methods of transdermal drug delivery systems: a review. *J Appl Pharm Res*, **9(2)**, 06–09 (2021) https://doi.org/10.18231/j.joapr.2021.06.09

[10] Morya N, Hirave K, Banerjee D, Singh A, Saharan VA. Herbal extracts and phytoconstituents-loaded transferosomes, ethosomes, and transdermal patches in drug delivery. In: *Formulating Pharma-, Nutra-, and Cosmeceutical Products from Herbal Substances*. 453–494 (2025) https://doi.org/10.1002/9781119769484.ch17

[11] Moezzi SM, Masoumi Shahrbabak S, Amiri S, Hajihosseini S, Masoudifar R, Mostafanejadian E, Akbari Javar H. Transdermal

drug delivery systems for psychological disorders. *Pharm Dev Technol*, **30(10)**, 1413–1448 (2025) https://doi.org/10.1080/10837450.2025.2576778

[12] Kulkarni P, Ahmed KA, Shirsand SB, Raikar PK, Hiraskar A. Transdermal patches: design, evaluation, and potential applications in modern therapeutics. *Biomed Mater Devices*, 1–9 (2025) https://doi.org/10.1007/s44174-025-00359-5

[13] Nagadev C, Rao M, Venkatesh P, Hepcykalarani D, Prema R. A review on transdermal drug delivery systems. *Asian J Res Pharm Sci*, **10(2)**, 109–114 (2020) https://doi.org/10.5958/2231-5659.2020.00021.1

[14] Shelke PV, Rachh PR, Mankar S, Amin S, Jain D. Optimization and evaluation of nebivolol hydrochloride-loaded transferosomes using Box–Behnken experimental design. *J Appl Pharm Res*, **12(4)**, 124–138 (2024) https://doi.org/10.69857/joapr.v12i4.590

[15] Tirkey F, Kori ML, Dwivedi A. Evaluation of wound healing potential of transdermal patches containing apigenin. *Biochem Cell Arch*, **24(2)** (2024) https://doi.org/10.51470/bca.2024.24.2.2281

[16] Trivedi D, Goyal A. Formulation and evaluation of transdermal patches containing dexketoprofen trometamol. *Int J Pharm Chem Anal*, **7(2)**, 87–97 (2020) https://doi.org/10.18231/j.ijpca.2020.014

[17] Nandi S, Mondal S. Fabrication and evaluation of matrix-type transdermal patch loaded with tramadol hydrochloride. *Turk J Pharm Sci*, **19(5)**, 572–579 (2022) https://doi.org/10.4274/tjps.galenos.2021.43678

[18] Shelke P V., Rachh PR, Mankar SD, Gorde PL. Optimization and Evaluation of Transdermal Delivery System for Nebivolol Hydrochloride. *J. Appl. Pharm. Res.*, **12**, 21–37 (2024) https://doi.org/10.69857/joapr.v12i3.580.

[19] Kim EJ, Choi DH. Quality by design approach to development of transdermal patch systems and regulatory perspective. *J Pharm Investig*, **51(6)**, 669–690 (2021) https://doi.org/10.1007/s40005-021-00536-w

[20] Shivalingam MR, Balasubramanian A, Ramalingam K. Design and evaluation of medicated dermal patches of esomeprazole. *Int J Pharm Res*, **12(4)** (2020) https://doi.org/10.31838/ijpr/2020.12.04.418

[21] Agrawal S, Gandhi SN, Gurjar P, Saraswathy N. Microneedles: an advancement to transdermal drug delivery system approach. *J Appl Pharm Sci*, **10(3)**, 149–159 (2020) https://doi.org/10.7324/JAPS.2020.103019

[22] Mummoorthy A, Karthikeyan A, Rajendran A, Suresh K, Balu A. Formulation, optimization, and in-vitro diffusion studies of novel niosomal gel of miconazole nitrate. *J Appl Pharm Res*, **14(2)**, 76–88 (2026) https://doi.org/10.69857/joapr.v14i2.1639

[23] Shivalingam MR, Balasubramanian AR, Ramalingam KO. Formulation and evaluation of transdermal patches of pantoprazole sodium. *Int J Appl Pharm*, **13(5)**, 287–291 (2021) https://doi.org/10.22159/ijap.2021v13i5.42175

[24] Tiwari R, Tiwari G, Singh R. Allopurinol-loaded transferosomes for alleviation of gout symptoms. *Curr Drug Ther*, **15(4)**, 404–419 (2020) https://doi.org/10.2174/1574885515666200120124214

[25] Neupane R, Boddu SH, Renukuntla J, Babu RJ, Tiwari AK. Alternatives to biological skin in permeation studies: current trends and possibilities. *Pharmaceutics*, **12(2)**, 152 (2020) https://doi.org/10.3390/pharmaceutics12020152

[26] Sivadasan D, Madkhali OA. Design features, quality by design approach, characterization, therapeutic applications, and clinical considerations of transdermal drug delivery systems: a comprehensive review. *Pharmaceuticals*, **17(10)**, 1346 (2024) https://doi.org/10.3390/ph17101346

[27] Riccio BV, Silvestre AL, Meneguin AB, Ribeiro TD, Klosowski AB, Ferrari PC, Chorilli M. Exploiting polymeric films as multipurpose drug delivery systems: a review. *AAPS PharmSciTech*, **23(7)**, 269 (2022) https://doi.org/10.1208/s12249-022-02414-6

[28] Antonara L, Triantafyllopoulou E, Chountoulesi M, Pippa N, Dallas PP, Rekkas DM. Lipid-based drug delivery systems: concepts and recent advances in transdermal applications. *Nanomaterials*, **15(17)**, 1326 (2025) https://doi.org/10.3390/nano15171326

[29] Elhabal SF, Ashour HA, Elrefai MF, Teaima MH, Elzohairy NA, El-Nabarawi M. Innovative transdermal delivery of microneedle patch for dual drugs febuxostat and lornoxicam in gouty arthritis. *J Drug Deliv Sci Technol*, **110**, 107053 (2025) https://doi.org/10.1016/j.jddst.2025.107053

[30] Manna S, Dhanalakshmi D, Bhowmik M, Jana S, Jana S. Cellulose derivative-based bioadhesive blend patch for transdermal drug delivery. *Front Mater*, **9**, 835507 (2022) https://doi.org/10.3389/fmats.2022.835507

[31] Kaur R, Arora S, Goswami M. Compatibility study of astaxanthin with pharmaceutical excipients for TDDS development. *AIP Conf Proc*, **3050(1)**, 050007 (2024) https://doi.org/10.1063/5.0194196

[32] Chen J, Liu X, Liu S, He Z, Yu S, Ruan Z, Jin N. Fabrication and characterization of dissolving microneedles for transdermal delivery of allopurinol. *Drug Dev Ind Pharm*, **47(10)**, 1578–1586 (2021) https://doi.org/10.1080/03639045.2022.2027959

[33] Buzia OD, Păduraru AM, Stefan CS, Dinu M, Cocoș DI, Nwabudike LC, Tatu AL. Strategies for improving transdermal administration: new approaches to controlled drug release. *Pharmaceutics*, **15(4)**, 1183 (2023) https://doi.org/10.3390/pharmaceutics15041183

[34] Nadendla RR, Priyanka PV. Optimizing transdermal patch formulation for enhanced rivaroxaban delivery using design of experiments. *Int J Pharm Pharm Sci*, **16(12)**, 8–20 (2024) https://doi.org/10.22159/ijpps.2024v16i12.51075

[35] Talole S, Godge R, Tambe N, Mhase N. Formulation and optimization of upadacitinib-loaded transdermal patches for rheumatoid arthritis with zero-order release kinetics. *J Appl Pharm Res*, **13(2)**, 181–193 (2025) https://doi.org/10.69857/joapr.v13i2.1037

[36] Nam SH. Transdermal delivery of risedronate using chemical enhancers for improved skin penetration. *J Appl Pharm Res*, **13(4)**, 45–52 (2025) https://doi.org/10.69857/joapr.v13i4.1013

[37] Yousuf M, Ahmad M, Naeem M, Khan MK, Khan BA. Development and in vitro evaluation of polymeric responsive release matrix-type transdermal patches of anti-asthmatic drugs. *Iran J Sci Technol Trans A Sci*, **45(1)**, 1–10 (2021) https://doi.org/10.1007/s40995-020-00985-2

[38] Kim S, Fouladian P, Afinjuomo F, Song Y, Youssef SH, Vaidya S, Garg S. Effect of plasticizers on drug-in-adhesive patches containing 5-fluorouracil. *Int J Pharm*, **611**, 121316 (2022) https://doi.org/10.1016/j.ijpharm.2021.121316

[39] Silva IR, Lima FA, Reis EC, Ferreira LA, Goulart GA. Stepwise protocols for preparation and use of porcine ear skin for in vitro skin permeation studies using Franz diffusion cells. *Curr Protoc*, **2(3)**, e391 (2022) https://doi.org/10.1002/cpz1.391

[40] Rapalli VK, Mahmood A, Waghule T, Gorantla S, Dubey SK, Alexander A, Singhvi G. Revisiting techniques to evaluate drug permeation through skin. *Expert Opin Drug Deliv*, **18(12)**, 1829–1842 (2021) https://doi.org/10.1080/17425247.2021.2010702

[41] Lal N, Verma N. Effect of acrylic polymers on transdermal patches: in vitro permeation and stability studies. *Future J Pharm Sci*, **7(1)**, 127 (2021) https://doi.org/10.1186/s43094-021-00272-w

[42] Shafique N, Siddiqui T, Zaman M, Iqbal Z, Rasool S, Ishaque A, Siddique W, Alvi MN. Transdermal patch co-loaded with pregabalin and ketoprofen for improved bioavailability. *Polym Polym Compos*, **29**, S376–S388 (2021) https://doi.org/10.1177/09673911211004516

[43] Sahu K, Pathan S, Khatri K, Upmanyu N, Shilpi S. Development and evaluation of antiemetic transdermal patches of ondansetron hydrochloride and dexamethasone. *GSC Biol Pharm Sci*, **14**, 067–078 (2021) https://doi.org/10.30574/gscbps.2021.14.3.0061

[44] Kriplani P, Guarve K, Baghel US. Formulation optimization and characterization of transdermal film of curcumin by response surface methodology. *Chin Herb Med*, **13(2)**, 274–285 (2021) https://doi.org/10.1016/j.chmed.2020.12.001

[45] Stamp LK, Chapman PT. Allopurinol hypersensitivity: pathogenesis and prevention. *Best Pract Res Clin Rheumatol*, **34(4)**, 101501 (2020) https://doi.org/10.1016/j.berh.2020.101501

[46] Alkilani AZ, Nasereddin J, Hamed R, Nimrawi S, Hussein G, Abo-Zour H, Donnelly RF. Beneath the skin: current trends and future prospects of transdermal drug delivery systems. *Pharmaceutics*, **14(6)**, 1152 (2022) https://doi.org/10.3390/pharmaceutics14061152

[47] Kumar V, Praveen N, Kewlani P, Arvind, Singh A, Rajamanickam VM. Transdermal drug delivery systems. In: *Advanced Drug Delivery: Methods and Applications*. Singapore: Springer Nature Singapore, 333–362 (2023) https://doi.org/10.1007/978-981-99-6564-9_13

[48] Gajbhiye SA, Ahire ED, Patil MP, Meshram PR, Patil YM. Polymers and their uses in drug delivery. In: *Pharmaceutical Polymer Formulations and Its Applications*. 181–206 (2025) https://doi.org/10.1002/9781394172856.ch7

[49] Kirk RD, Akanji T, Li H, Shen J, Allababidi S, Seeram NP, Bertin MJ, Ma H. Evaluation of skin permeability of cannabidiol formulations using Franz diffusion assay. *Med Cannabis Cannabinoids*, **5(1)**, 129–137 (2022) https://doi.org/10.1159/000526769

[50] Kumar M, Sharma A, Mahmood S, Thakur A, Mirza MA, Bhatia A. Franz diffusion cell and its implication in skin permeation studies. *J Dispersion Sci Technol*, **45(5)**, 943–956 (2024) https://doi.org/10.1080/01932691.2023.2188923

[51] Yewale C, Tandel H, Patel A, Misra A. Polymers in transdermal drug delivery. In: *Applications of Polymers in Drug Delivery*. Elsevier, 131–158 (2021) https://doi.org/10.1016/B978-0-12-819659-5.00005-7

[52] Kusum Devi V, Saisivam S, Maria GR, Deepti PU. Design and evaluation of matrix diffusion-controlled transdermal patches of verapamil hydrochloride. *Drug Dev Ind Pharm*, **29(5)**, 495–503 (2003) https://doi.org/10.1081/DDC-120018638

[53] Adepu S, Ramakrishna S. Controlled drug delivery systems: current status and future directions. *Molecules*, **26(19)**, 5905 (2021) https://doi.org/10.3390/molecules26195905

[54] Kim K, Kim HS, Hwang MJ, Lee CM, Choe SW, Lee W, Jeong KC, Yoon SD. Controlled drug release properties of allopurinol-incorporated double-layered chitosan/starch patches for gout therapy. *Colloids Surf B Biointerfaces*, 115054 (2025) https://doi.org/10.1016/j.colsurfb.2025.115054